IEEE Access
Multidisciplinary | Rapid Review | Open Access Journal

Received October 19, 2019, accepted October 27, 2019, date of publication November 4, 2019, date of current version November 14, 2019.

Digital Object Identifier 10.1109/ACCESS.2019.2951173

Accurate and Efficient Finite-Difference Time-Domain Simulation Compared With CCPR Model for Complex Dispersive Media

HONGJIN CHOI, YEON-HWA KIM, JAE-WOO BAEK, AND KYUNG-YOUNG JUNG, (Senior Member, IEEE)
Department of Electronics and Computer Engineering, Hanyang University, Seoul 04763, South Korea

Corresponding author: Kyung-Young Jung (kyjung3@hanyang.ac.kr)

This work was supported by the Research Fund of Signal Intelligence Research Center, Supervised by Defense Acquisition Program Administration and Agency for Defense Development of Korea.

ABSTRACT Recently, it has received a great deal of attention to analyze the electromagnetic wave problems in dispersive media by using the finite-difference time-domain (FDTD) method. Accordingly, it is of great importance to employ a proper dispersion model which can fit the frequency-dependent permittivity of a medium considered. The reported dispersion models include Debye, Drude, Lorentz, modified Lorentz, quadratic complex rational function, complex-conjugate pole-residue (CCPR) models. The CCPR dispersion model has advantage over other dispersion models in the fact that accurate CCPR dispersion parameters can be simply extracted by using the powerful and robust vector fitting tool which has been widely used in the circuit theory. However, the arithmetic operation of CCPR-based FDTD implementation is involved with complex-valued numbers and thus its numerical computation is not efficient. In this work, we propose an accurate and efficient FDTD simulation for complex dispersive media. In specific, an accurate CCPR dispersion model is simply obtained using the vector fitting tool and then the CCPR dispersion model is converted to the modified Lorentz dispersion model which leads to the arithmetic operation of only real-valued numbers in its FDTD implementation. Numerical examples are used to illustrate the accuracy and efficiency of our dispersive FDTD simulation.

INDEX TERMS Dispersion model, dispersive media, finite-difference time-domain (FDTD) method, human tissue, plasmonics.

I. INTRODUCTION

The finite-difference time-domain (FDTD) method has been popularly employed to analyze a variety of electromagnetic (EM) wave problems because of its simplicity, robustness, and accuracy [1]–[4]. For exmaple, FDTD method was successfully employed for complex dispersive media [5]–[7]. Until now, a variety of dispersion models to fit the frequency-dependent permittivity has been introduced such as Debye, Drude, Lorentz, modified Lorentz, quadratic complex rational function (QCRF), and complex-conjugate pole-residue (CCPR) models [8]–[16]. For biological tissues, the Cole-Cole model [17] or high-order Debye model [18] has been widely used. However, for the Cole-Cole model, the computational costs of its FDTD implementation are overwhelmingly huge because the fractional order differentiator is involved with FDTD update equations [19]. For the high-order Debye model, complicated optimization techniques are needed to extract Debye parameters. Proper initial values should be employed to yield accurate modeling, otherwise it may lead to inaccurate modeling [20].

Alternatively, the CCPR dispersion model can be accurately obtained with the help of the powerful and robust vector fitting technique [21] which is really easy to use and also freely available [22]. Differently from other dispersion models, initial values are not needed in the CCPR dispersion model. There are various FDTD methods for dispersive media, including recursive convolution, piecewise linear recursive convolution, Z transform, and auxiliary differential equation (ADE) methods [23]–[25]. The ADE-FDTD method can be used to obtain simpler arithmetic operations than others and it can be also extended to nonlinear dispersive media problems [12]. The CCPR dispersion model is widely used with ADE-FDTD method

The associate editor coordinating the review of this manuscript and approving it for publication was Mengmeng Li.

TABLE 1. Pros and cons of various FDTD dispersion models.

Model	Advantage	Disadvantage
Debye Drude Lorentz	Well established and widely used	Involved with a complicated optimization technique (accurate fitting may fail for improper initial guess.)
QCRF	Accurate and efficient	Not straightforward to extend to multi-term cases
Cole-Cole	Well suitable for biological tissues	Overwhelming FDTD implementation costs (due to the fractional order differentiator)
CCPR	Easy and accurate parameter extraction (using the vector fitting tool)	Inefficient FDTD implementation (due to complex-valued variables)
modified Lorentz	Accurate and efficient Easy conversion from the CCPR model	Involved with a complicated optimization technique (accurate fitting may fail for improper initial guess.)

due to the complex conjugate property of auxiliary variables. When the ADE-FDTD method is applied to the CCPR dispersion model, the resulting FDTD simulation should treat complex-valued variables. Therefore, the computational costs of CCPR-based FDTD simulations are not efficient, although the formulation of CCPR-FDTD seems to be simple.

The dispersion model consisting only of real-valued parameters is highly necessary to efficiently simulate dispersive media using the FDTD method. In the aspect of accuracy, the degree of freedom of the modified Lorentz and QCRF dispersion models is greater than Debye, Drude, and Lorentz models. The formulation of QCRF-based FDTD is based on the constitutive relation between the electric flux density and the electric field, so that it is not straightforward to extend to multi-pole cases. On the other hand, modified Lorentz-based FDTD can be easily extended to multi-term cases by the constitutive relation between the current density and the electric field. In addition, the parameters of the modified Lorentz dispersion model can be obtained by converting the CCPR dispersion model with simple mathematical manipulations. Pros and cons of aforementioned FDTD dispersion models are summarized in Table 1.

In this work, we propose an accurate and efficient FDTD simulation for complex dispersive media based on the modified Lorentz-FDTD formulation converted from the CCPR dispersion model. It will be shown that the number of arithmetic operations for modified Lorentz-FDTD is less than the CCPR-FDTD counterpart by investigating their FDTD formulations. Finally, various numerical examples are employed to illustrate the accuracy and efficiency of the proposed FDTD simulation for complex dispersive media.

II. FDTD FORMULATIONS

The main idea of our work is to perform FDTD update based on the modified Lorentz model which is converted from CCPR parameters. To sum up, the proposed dispersive-FDTD procedure is as follows:

i) To extract the CCPR parameters by using the powerful and robust vector fitting tool.

ii) To convert the parameters of the CCPR model to those of the modified Lorentz model (by the relation that will be presented).

iii) To proceed the dispersive-FDTD update based on the modified Lorentz model.

In followings, we quantitatively compare the computational efficiency of CCPR-FDTD and the modified Lorentz counterpart in detail.

In what follows, an $e^{j\omega t}$ time dependence is assumed. For nonmagnetic materials, the update equation of the magnetic field $\mathbf{H}$ can be derived by applying the conventional central difference scheme (CDS) to Faraday's law and the resulting FDTD update equation is

$$\mathbf{H}^{n+1/2} = \mathbf{H}^{n-1/2} - \frac{\Delta_t}{\mu_0}\nabla \times \mathbf{E}^n, \tag{1}$$

where μ_0 is the magnetic permeability of the free space, Δ_t denotes the FDTD time step size, and the superscript indicates the time index. In this work, the update equation of CCPR-FDTD and the modified Lorentz counterpart will be obtained by using the relation between the current field, $\mathbf{J}$, and electric field, $\mathbf{E}$, which is originated from Ampere's law in the frequency domain,

$$\nabla \times \mathbf{H}(\omega) = j\omega\varepsilon_0\varepsilon_r(\omega)\mathbf{E}(\omega), \tag{2}$$

where ε_0 is the electric permittivity of the free space, $\varepsilon_r(\omega) = \varepsilon_{r,\infty} + \chi(\omega)$, and $\varepsilon_{r,\infty}$ is relative permittivity at infinite frequency. The constitutive relation between $\mathbf{J}$ field and $\mathbf{E}$ field is

$$\mathbf{J}(\omega) = j\omega\varepsilon_0\chi(\omega)\mathbf{E}(\omega). \tag{3}$$

A. CCPR-FDTD

The relative permittivity of the CCPR model can be expressed as

$$\varepsilon_r(\omega) = \varepsilon_{r,\infty} + \sum_{q=1}^{M}\left(\frac{r_q}{j\omega - p_q} + \frac{r_q^*}{j\omega - p_q^*}\right). \tag{4}$$

By the constitutive relation, we can express as

$$\mathbf{J}_q(\omega) = j\omega\varepsilon_0\frac{r_q}{j\omega - p_q}\mathbf{E}(\omega), \tag{5}$$

$$\mathbf{J}_q^c(\omega) = j\omega\varepsilon_0\frac{r_q^*}{j\omega - p_q^*}\mathbf{E}(\omega). \tag{6}$$

By converting the frequency domain into the time domain, it is known that $\mathbf{J}_q(t)$ and $\mathbf{J}_q^c(t)$ are conjugate pair. Therefore, it suffices to store only one component of current field, $\mathbf{J}_q$. The update equation of $\mathbf{J}_q$ can be obtained by applying inverse Fourier transform (IFT) and CDS to the constitutive relation (5),

$$\mathbf{J}_q^{n+1} = k_q \mathbf{J}_q^n + \beta_q \frac{\mathbf{E}^{n+1} - \mathbf{E}^n}{\Delta_t}, \tag{7}$$

where

$$k_q = \frac{1 + p_q \Delta_t/2}{1 - p_q \Delta_t/2} \quad \text{and } \beta_q = \frac{\varepsilon_0 r_q \Delta_t}{1 - p_q \Delta_t/2}. \tag{8}$$

The $\mathbf{E}$ field can be updated by applying IFT and CDS to Ampere's law (2),

$$\nabla \times \mathbf{H}^{n+1/2} = \varepsilon_\infty \frac{\mathbf{E}^{n+1} - \mathbf{E}^n}{\Delta_t} + 2\mathrm{Re}\left(\sum_{q=1}^{M} \mathbf{J}_q^{n+1/2} \right), \tag{9}$$

where $\varepsilon_\infty = \varepsilon_0 \varepsilon_{r,\infty}$.
The $\mathbf{J}$ field at $(n+1/2)\Delta_t$ is not defined. Therefore, $\mathbf{J}_q^{n+1/2} \simeq 0.5(\mathbf{J}_q^{n+1} + \mathbf{J}_q^n)$ is used. The update equation of $\mathbf{E}$ field can be obtained by combining the auxiliary differential equation (7) with Ampere's law (9),

$$\mathbf{E}^{n+1} = \mathbf{E}^n + \frac{\Delta_t}{\varepsilon_\infty + \sum_{q=1}^{M} \mathrm{Re}(\beta_q)} \left[\nabla \times \mathbf{H}^{n+1/2} - \mathrm{Re}\left(\sum_{q=1}^{M} (k_q + 1) \mathbf{J}_q^n \right) \right]. \tag{10}$$

Note that when the parameters of the CCPR dispersion model are real-valued numbers, the last term (the complex conjugate term) in (4) disappears and thus this dispersion model is equivalent to the Debye model. In this case, the update equation of electric field $\mathbf{E}$ can be

$$\mathbf{E}^{n+1} = \mathbf{E}^n + \frac{\Delta_t}{\varepsilon_\infty + \sum_{q=1}^{M} \beta_q/2} \left[\nabla \times \mathbf{H}^{n+1/2} - \left(\sum_{q=1}^{M} \frac{k_q + 1}{2} \mathbf{J}_q^n \right) \right]. \tag{11}$$

To unify above two update equations, let us introduce new FDTD coefficients B_q and K_q. Note that $B_q = 0.5\beta_q$ for the real parameter and $B_q = \beta_q$ for the complex parameter. In the similar manner, K_q indicates $0.5(k_q + 1)$ for the real parameter or $(k_q + 1)$ for the complex parameter. The final update equation of $\mathbf{E}$ field is

$$\mathbf{E}^{n+1} = \mathbf{E}^n + \frac{\Delta_t}{\varepsilon_\infty + \sum_{q=1}^{M} \mathrm{Re}(B_q)} \left[\nabla \times \mathbf{H}^{n+1/2} - \mathrm{Re}\left(\sum_{q=1}^{M} K_q \mathbf{J}_q^n \right) \right]. \tag{12}$$

The update procedures are as follows: update the magnetic field $\mathbf{H}$ by using the Faraday's law (1). After updating the electric field $\mathbf{E}$ based on Ampere's law (12), update the current field $\mathbf{J}$ by the constitutive relation between $\mathbf{E}$ and $\mathbf{J}$ (7).

TABLE 2. The number of arithmetic operations for CCPR-FDTD (per computational cell and field component).

update	A/S		M/D		
	real	complex	real	complex	real&complex
E_x	5	$M-1$	2	M	0
J_x	M	M	0	M	M

Let us consider the number of arithmetic operations in updating one component of $\mathbf{E}$ and $\mathbf{J}$ (e.g., E_x and J_x). In practical FDTD simulation, all multiplicative factors are precomputed before FDTD time marching [26]. For example, the update equation of E_x is

$$\begin{aligned} E_x|_{i+1/2,j,k}^{n+1} = E_x|_{i+1/2,j,k}^{n} &- \mathrm{Re}\left(\sum_{q=1}^{M} \left(C_{1,q} J_{x,q}|_{i+1/2,j,k}^{n} \right) \right) \\ &+ C_2 \left(H_z|_{i+1/2,j+1/2,k}^{n+1/2} - H_z|_{i+1/2,j-1/2,k}^{n+1/2} \right) \\ &- C_3 \left(H_y|_{i+1/2,j,k+1/2}^{n+1/2} - H_y|_{i+1/2,j,k-1/2}^{n+1/2} \right), \end{aligned} \tag{13}$$

where

$$C_{1,q} = \frac{K_q \Delta_t}{\varepsilon_\infty + \sum_{q=1}^{M} \mathrm{Re}(B_q)}, \quad C_2 = \frac{1}{\Delta_y} \frac{\Delta_t}{\varepsilon_\infty + \sum_{q=1}^{M} \mathrm{Re}(B_q)}$$
$$C_3 = \frac{1}{\Delta_z} \frac{\Delta_t}{\varepsilon_\infty + \sum_{q=1}^{M} \mathrm{Re}(B_q)}. \tag{14}$$

Note that the subscript denotes the space index. To update one component of $\mathbf{E}$ field, five addition and subtraction (A/S) of real-valued numbers and $(M-1)$ A/S of complex-valued numbers are required, while two multiplication and division (M/D) of real-valued numbers and M M/D of complex-valued numbers are required. The required number of arithmetic operation to update one component of $\mathbf{J}$ field can be found by following the similar procedures as the update equation of $\mathbf{E}$. It is listed on Table 2. For updating one component of $\mathbf{E}$ and $\mathbf{J}$, two real-valued field variables (E_x^{n+1} and E_x^n) and M complex-valued field variables ($J_{x,q}^n$) are required. Note that memory storage for $J_{x,q}^{n+1}$ is not required since it can overwrite its previous value.

B. MODIFIED LORENTZ-FDTD

The modified Lorentz model can be simply converted from the CCPR model, as alluded to earlier. The conversion procedure should be performed separately whether the CCPR parameter is complex-valued or real-valued. Toward this purpose, the CCPR model can be written as

$$\varepsilon_{r,\infty} + \sum_{q=1}^{M_C} \left(\frac{r_q}{j\omega - p_q} + \frac{r_q^*}{j\omega - p_q^*} \right) + \sum_{q=1}^{M_R} \frac{r_{M_C+q}}{j\omega - p_{M_C+q}}, \tag{15}$$

where M_C denotes the number of complex-valued parameters, M_R real-valued parameters, and $M_C + M_R = M$.

The modified Lorentz model can be expressed as

$$\varepsilon_r(\omega) = \varepsilon_{r,\infty} + \sum_{q=1}^{N} \frac{a_{0,q} + a_{1,q}(j\omega)}{b_{0,q} + b_{1,q}(j\omega) + b_{2,q}(j\omega)^2}, \quad (16)$$

where N is the number of modified Lorentz terms which will be mentioned later. The modified Lorentz parameters can be converted from the CCPR term with complex parameters ($q \le M_C$) as

$$\begin{aligned} a_{0,q} &= -2\mathrm{Re}(p_q r_q^*), \quad a_{1,q} = 2\mathrm{Re}(r_q), \\ b_{0,q} &= |p_q|^2, \quad b_{1,q} = -2\mathrm{Re}(p_q), \; b_{2,q} = 1. \end{aligned} \quad (17)$$

For the real parameters of the CCPR model ($q > M_C$), the modified Lorentz parameters can be easily obtained by combining two CCPR terms with real parameters simultaneously:

$$\begin{aligned} a_{0,q} &= -(p_{2q-M_C-1} r_{2q-M_C} + p_{2q-M_C} r_{2q-M_C-1}), \\ a_{1,q} &= r_{2q-M_C-1} + r_{2q-M_C}, \, b_{0,q} = p_{2q-M_C-1} p_{2q-M_C}, \\ b_{1,q} &= -(p_{2q-M_C-1} + p_{2q-M_C}), \quad b_{2,q} = 1. \end{aligned} \quad (18)$$

For odd-numbered M_R, there exists one remaining CCPR term with real-valued parameters and the equivalent modified Lorentz parameters can be simply written as

$$\begin{aligned} a_{0,N} &= r_M, \quad a_{1,N} = 0, \\ b_{0,N} &= -p_M, \quad b_{1,N} = 1, \; b_{2,N} = 0. \end{aligned} \quad (19)$$

Note that $N = M - M_R/2$ for even-numbered M_R or $N = M - M_R/2 + 1/2$ for odd-numbered M_R.

For the update equations of modified Lorentz-FDTD, we consider Ampere's law (2) and the constitutive relation between $\mathbf{E}$ and $\mathbf{J}$ (3):

$$\nabla \times \mathbf{H}^{n+1/2} = \varepsilon_\infty \frac{\mathbf{E}^{n+1} - \mathbf{E}^n}{\Delta_t} + \sum_{q=1}^{N} \mathbf{J}_q^{n+1/2}, \quad (20)$$

$$\mathbf{J}_q = j\omega\varepsilon_0 \frac{a_{0,q} + a_{1,q}(j\omega)}{b_{0,q} + b_{1,q}(j\omega) + b_{2,q}(j\omega)^2} \mathbf{E}. \quad (21)$$

To update the $\mathbf{J}$ field, IFT and CDS are applied. In addition, double averaging scheme [8], [27] is applied to the zeroth order term,

$$f \longrightarrow \frac{f^{n+1} + 2f^n + f^{n-1}}{4}. \quad (22)$$

Therefore, the final update equation of $\mathbf{J}$ field can be obtained

$$\begin{aligned} C_{a,q}\mathbf{J}_q^{n+1} + C_{b,q}\mathbf{J}_q^n + C_{c,q}\mathbf{J}_q^{n-1} \\ = C_{d,q}\mathbf{E}^{n+1} + C_{e,q}\mathbf{E}^n + C_{f,q}\mathbf{E}^{n-1}, \end{aligned} \quad (23)$$

where

$$\begin{aligned} C_{a,q} &= b_{0,q}\Delta_t^2 + 2b_{1,q}\Delta_t + 4b_{2,q}, \\ C_{b,q} &= 2b_{0,q}\Delta_t^2 - 8b_{2,q}, \\ C_{c,q} &= b_{0,q}\Delta_t^2 - 2b_{1,q}\Delta_t + 4b_{2,q}, \\ C_{d,q} &= 2a_{0,q}\varepsilon_0\Delta_t + 4a_{1,q}\varepsilon_0, \\ C_{e,q} &= -8a_{1,q}\varepsilon_0, \quad C_{f,q} = -2a_{0,q}\varepsilon_0\Delta_t + 4a_{1,q}\varepsilon_0. \end{aligned} \quad (24)$$

The update equation of $\mathbf{E}$ can be obtained by combining the above auxiliary equation (23) with Ampere's law (20),

$$\begin{aligned} &\left(\frac{\varepsilon_\infty}{\Delta_t} + \sum_{q=1}^{N} \frac{C_{d,q}}{2C_{a,q}}\right)\mathbf{E}^{n+1} \\ &= \left(\frac{\varepsilon_\infty}{\Delta_t} - \sum_{q=1}^{N} \frac{C_{e,q}}{2C_{a,q}}\right)\mathbf{E}^n \\ &\quad - \left(\sum_{q=1}^{N} \frac{C_{f,q}}{2C_{a,q}}\right)\mathbf{E}^{n-1} + \nabla \times \mathbf{H}^{n+1/2} \\ &\quad + \sum_{q=1}^{N} \frac{C_{b,q} - C_{a,q}}{2C_{a,q}}\mathbf{J}_q^n + \sum_{q=1}^{N} \frac{C_{c,q}}{2C_{a,q}}\mathbf{J}_q^{n-1}. \end{aligned} \quad (25)$$

The update procedures of modified Lorentz-FDTD are same as the CCPR counterpart. The required number of arithmetic operations of modified Lorentz-FDTD is less than the CCPR counterpart because the former contains only real-valued variables. For example, the update equation of E_x is

$$\begin{aligned} &E_x|_{i+1/2,j,k}^{n+1} \\ &= C_1 E_x|_{i+1/2,j,k}^{n} - C_2 E_x|_{i+1/2,j,k}^{n-1} \\ &\quad + C_3\left(H_z|_{i+1/2,j+1/2,k}^{n+1/2} - H_z|_{i+1/2,j-1/2,k}^{n+1/2}\right) \\ &\quad - C_4\left(H_y|_{i+1/2,j,k+1/2}^{n+1/2} - H_y|_{i+1/2,j,k-1/2}^{n+1/2}\right) \\ &\quad + \sum_{q=1}^{N}\left(C_{5,q} J_{x,q}|_{i+1/2,j,k}^{n}\right) + \sum_{q=1}^{N}\left(C_{6,q} J_{x,q}|_{i+1/2,j,k}^{n-1}\right), \end{aligned} \quad (26)$$

where

$$\begin{aligned} C_1 &= \frac{\frac{\varepsilon_\infty}{\Delta_t} - \sum_{q=1}^{N}\frac{C_{e,q}}{2C_{a,q}}}{\frac{\varepsilon_\infty}{\Delta_t} + \sum_{q=1}^{N}\frac{C_{d,q}}{2C_{a,q}}}, \quad C_2 = \frac{\sum_{q=1}^{N}\frac{C_{f,q}}{2C_{a,q}}}{\frac{\varepsilon_\infty}{\Delta_t} + \sum_{q=1}^{N}\frac{C_{d,q}}{2C_{a,q}}}, \\ C_3 &= \frac{1}{\Delta_y}\frac{1}{\frac{\varepsilon_\infty}{\Delta_t} + \sum_{q=1}^{N}\frac{C_{d,q}}{2C_{a,q}}}, \quad C_4 = \frac{1}{\Delta_z}\frac{1}{\frac{\varepsilon_\infty}{\Delta_t} + \sum_{q=1}^{N}\frac{C_{d,q}}{2C_{a,q}}}, \\ C_{5,q} &= \frac{\frac{C_{b,q} - C_{a,q}}{2C_{a,q}}}{\frac{\varepsilon_\infty}{\Delta_t} + \sum_{q=1}^{N}\frac{C_{d,q}}{2C_{a,q}}}, \quad C_{6,q} = \frac{\frac{C_{c,q}}{2C_{a,q}}}{\frac{\varepsilon_\infty}{\Delta_t} + \sum_{q=1}^{N}\frac{C_{d,q}}{2C_{a,q}}}. \end{aligned} \quad (27)$$

The number of arithmetic operations of modified Lorentz-FDTD is listed on Table 3. In terms of memory costs, three real-valued variables (E_x^{n+1}, E_x^n, and E_x^{n-1}) and $2N$ real-valued variables ($J_{x,q}^n$ and $J_{x,q}^{n-1}$) are required per computational cell and $\mathbf{E}$ and $\mathbf{J}$ field components. Note that memory storage for $J_{x,q}^{n+1}$ is not required since it can overwrite its previous value.

It is not straightforward to compare the number of arithmetic operations of the both FDTD formulations because CCPR-FDTD contains complex-valued operations but modified Lorentz-FDTD performs only real-valued operations. Let us consider the operation of two complex-valued numbers. One A/S of two complex-valued numbers contains

TABLE 3. The number of arithmetic operations for modified Lorentz-FDTD (per computational cell and field component).

update	A/S	M/D
E_x	$2N+5$	$2N+4$
J_x	$4N$	$5N$

TABLE 4. Computational efficiency based on real-valued numbers (per computational cell and E and J field components).

Implementation	Operation Count		Variables
	A/S	M/D	
CCPR	$9M+3$	$10M+2$	$2M+2$
modified Lorentz	$6N+5$	$7N+4$	$2N+3$

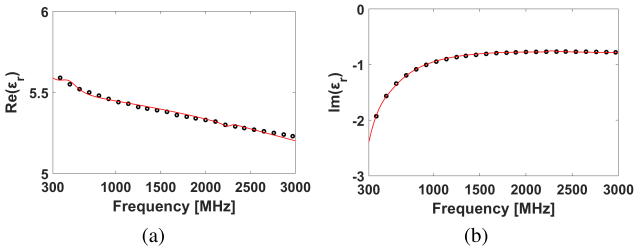

FIGURE 1. Complex permittivity of human fat. Red solid lines indicate the fitted curve dispersion model and black circles indicate Gabriel's dielectric properties provided by IFAC [28].

two A/S, while M/D of those does two A/S and four M/D. To sum up, Table 4 shows the required number of *real-valued* arithmetic operations in terms of E_x and J_x. It can be found out that the number for updating CCPR-FDTD listed in Table 4 grows faster than the modified Lorentz counterpart as the number of poles increases. It is also important to compare CCPR-FDTD with modified Lorentz-FDTD in terms of memory requirement. Note that one complex-valued variable should be assigned to two real-valued memory. As shown in Table 4, $2M+2$ and $2N+3$ real-valued memory allocations are required for CCPR-FDTD and modified Lorentz-FDTD respectively (per computational cell and **E** and **J** field components).

III. NUMERICAL EXAMPLES

In this section, FDTD simulations are performed for the CCPR dispersion model and the modified Lorentz model, highlighting the comparison of their computational efficiency. All FDTD simulations are performed on Intel i7-6700 CPU. First, let us consider an inhomogenous one-dimensional (1-D) case of human fat in the frequency range of 0.3–3 GHz. The complex relative permittivity of human fat can be found in [28]. The CCPR parameters are easily obtained by the powerful vector fitting tool [22] and they are listed in Table 5. As shown in Fig. 1, the vector fitting algorithm is accurate to extract the CCPR parameters. Note that the modified Lorentz parameters are obtained from the CCPR parameters, as mentioned previously. For the 1-D FDTD simulations, the space step size $\Delta_z = 1$ *mm*, the time step

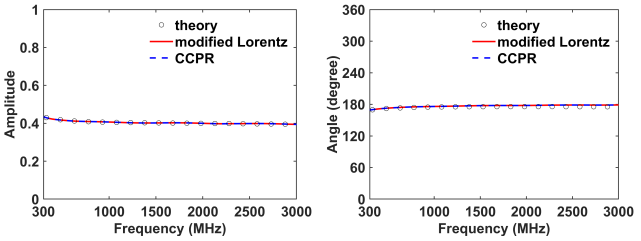

FIGURE 2. 1-D FDTD simulation results for human fat in 0.3–3 GHz. (a) Amplitude of reflection coefficient. (b) Angle of reflection coefficient.

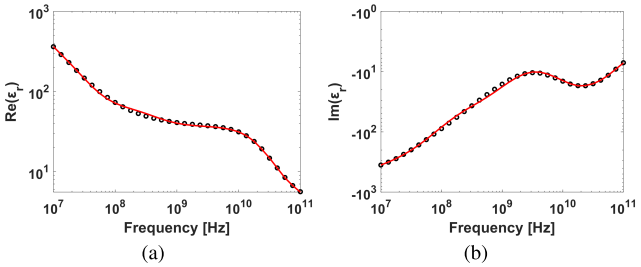

FIGURE 3. Complex permittivity of human dry skin. Red solid lines indicate the fitted curve dispersion model and black circles indicate Gabriel's dielectric properties provided by IFAC [28].

size $\Delta_t = C_n\Delta_z/c_0$, and the Courant number $C_n = 0.99$ are employed. Note that $c_0 = 1/\sqrt{\mu_0\varepsilon_0}$ and the maximum time step size Δ_t is derived by applying von Neumann method to satisfy the numerical stability condition [29]. The Gaussian-modulated sinewave is excited in the freespace and the computational domain of 10,000 FDTD cells is truncated by the 10 layer of perfectly matched layer (PML) [2]. To compare the 1-D FDTD results with theory [30], the reflection coefficient is obtained. The reflection coefficient for the two FDTD simulations is same to each other and both simulations yield accurate result compared to the theoretical value as shown in Fig. 2. The CPU time of CCPR-FDTD is approximately 44 % slower than that of the modified Lorentz counterpart.

Next, we consider a homogenous two-dimensional (2-D) problem. The vector fitting tool is again used to extract the CCPR parameters of human dry skin from 10 MHz to 100 GHz [28]. The extracted CCPR parameters are found in Table 5. As shown in Fig. 3, the CCPR dispersion model agrees very well with Gabriel's data [28]. In this 2-D example, the FDTD space step size $\Delta_x = \Delta_y = 0.55$ *mm* and the time step size $\Delta_t = C_n/\left(c_\infty\sqrt{1/\Delta_x^2 + 1/\Delta_y^2}\right)$ are employed and the other conditions are the same as the 1-D case. Note that $c_\infty = 1/\sqrt{\mu_0\varepsilon_\infty}$. As shown in Fig. 4, both FDTD simulations of human dry skin are same. The CCPR-FDTD simulation takes longer time approximately 66 % than the modified Lorentz-FDTD simulation in this example. In addition, the latter has advantage about 23% over the former in the aspect of the memory cost as can be expected from Table 4.

As a final example, a 3-D Au nanosphere with the radius of 40 nm is placed at the center of the FDTD computational domain of 150×150×150. The CCPR dispersion

TABLE 5. CCPR parameters of numerical examples.

Material	Fat	Dry skin	Au [31]
$\varepsilon_{r,\infty}$	4.115448	3.898214	1.366
p_1	-8.374186e+08 +j3.032112e+09	-3.109728e+10 +j1.392365e+11	-5.6511e+05 -j1.4394e+14
r_1	5.923876e+07 -j1.122860e+07	1.286981e+10 -j1.640851e+09	3.5070e+15 +j5.6374e+17
p_2	-3.029324e+08 +j1.419929e+10	-7.699466e+10 +j4.583800e+11	-2.6075e+05 -j1.5757e+15
r_2	3.990040e+06 +j5.144260e+06	5.266720e+09 +j1.232239e+10	2.0574e+14 +j1.0700e+14
p_3	-6.700849e+07	-2.512591e+09	-3.2320e+14 -j3.8109e+15
r_3	4.420158e+09	6.161072e+10	4.7956e+14 -j3.2670e+13
p_4	-3.737597e+10	-1.411084e+11	-1.5803e+15 -j3.5830e+15
r_4	5.082420e+10	4.641218e+12	9.3313e+15 -j4.4765e+14
p_5		-3.268712e+07	
r_5		2.330353e+10	
p_6		-1.524569e+08	
r_6		2.684338e+10	

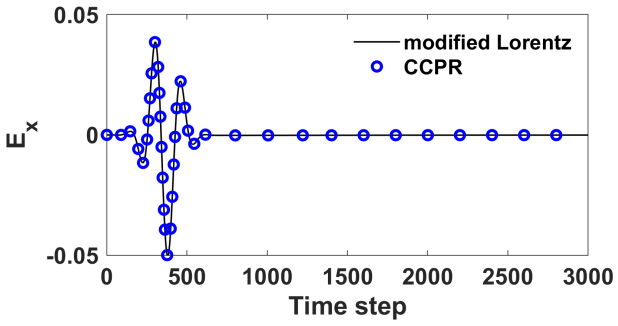

FIGURE 4. 2-D FDTD simulation results for dry skin in 10 MHz–100 GHz.

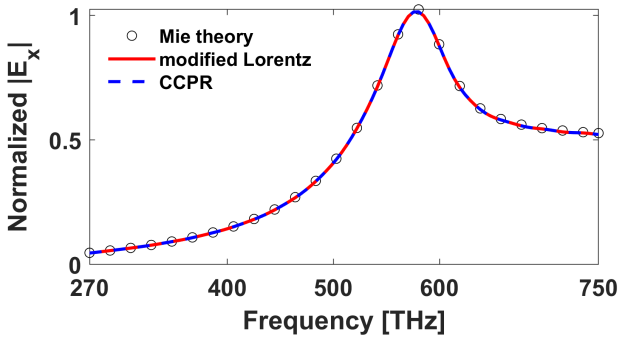

FIGURE 5. 3-D FDTD simulation results for Au in 270–750 THz.

model for Au is adopted from [31]. The space step size $\Delta_x = \Delta_y = \Delta_z = 1$ *nm* and the time step size $\Delta_t = C_n/\left(c_0\sqrt{1/\Delta_x^2 + 1/\Delta_y^2 + 1/\Delta_z^2}\right)$ are used. The total number of time marching step is 20,000. An x-polarized Gaussian-modulated sinewave on the xy plane is excited and the 10-layer complex frequency shifted (CFS)-PML [2], [32] is used to terminate the computational domain. The magnitude of E_x at the center of the sphere normalized by the incident field is calculated for the comparison of Mie theory [33]. Fig. 5 shows the spectral response of the normalized E_x. As shown in Fig. 5, the results of the two FDTD formulations agree well with each other and both are accurate compared to the Mie theory. It takes 7.25 hours for the CCPR simulation, while only 6.17 hours for the modified Lorentz counterpart. For the memory cost, the former takes less memory about 8 % than the latter because the CCPR parameters only consist of complex-valued number. The CPU time and memory requirement for three numerical examples are summarized in Table 6.

It is worth discussing the CPU time acceleration of modified Lorentz-FDTD against CCPR-FDTD in more details. In all numerical examples presented above, the computational time of modified Lorentz-FDTD is superior to that of CCPR-FDTD. This can be inferred from the number of arithmetic operation count in Table 4. For example, in the very first problem (1-D human fat), the total numbers of A/S

TABLE 6. Computational efficiency.

material	FDTD simulation	CPU time	Memory (MB)
Fat	modified Lorentz	3.85 s	7
	CCPR	5.56 s	7.1
Dry skin	modified Lorentz	144.71 s	107.6
	CCPR	240.87 s	132.2
Au	modified Lorentz	6.17 h	1637.8
	CCPR	7.25 h	1512.5

and M/D for updating **E** and **J** are 39 and 42 respectively for CCPR-FDTD, while those for modified Lorentz-FDTD are 23 and 25 respectively. However, the ratio of the arithmetic operation count number cannot exactly indicate the gain in the FDTD simulation speed up. In actual FDTD simulations, the FDTD time-marching procedure contains update of **H** and also additional auxiliary variables should be updated in the PML region. In addition, the actual FDTD computation time depends on the memory access time and the volume fraction of dispersive media.

IV. CONCLUSION

We have proposed accurate and efficient FDTD simulation for complex dispersive media. The accurate coefficients of the CCPR dispersion model are extracted by applying the state-of-art vector fitting tool. The CCPR parameters are converted to the modified Lorentz parameters in order to enhance the computational efficiency of FDTD simulations. The number of arithmetic operations of CCPR-FDTD and modified Lorentz-FDTD formulations are computed to elucidate the higher speed of modified Lorentz-FDTD simulation time against the CCPR-FDTD counterpart. The memory requirement is also compared between CCPR-FDTD and modified Lorentz-FDTD. Numerical examples are employed to illustrate the accuracy and efficiency of the proposed dispersive FDTD simulation in the EM analysis of human tissues and Au in a wide range of frequencies. The proposed FDTD simulation can be extended to a variety of complex dispersive media.

REFERENCES

[1] A. Taflove and S. C. Hagness, *Computational Electrodynamics: The Finite-Difference Time-Domain Method*, 3rd ed. Norwood, MA, USA: Artech House, 2005.

[2] S. D. Gedney, *Introduction to the Finite-Difference Time-Domain (FDTD) Method for Electromagnetics*. Lexington, KY, USA: Morgan & Claypool, 2010.

[3] S.-G. Ha, J. Cho, J. Lee, B.-W. Min, J. Choi, and K.-Y. Jung, "Numerical study of estimating the arrival time of UHF signals for partial discharge localization in a power transformer," *J. Electromagn. Eng. Sci.*, vol. 18, no. 2, pp. 94–100, Apr. 2018.

[4] J.-W. Baek, D.-K. Kim, and K.-Y. Jung, "Finite-difference time-domain modeling for electromagnetic wave analysis of human voxel model at millimeter-wave frequencies," *IEEE Access*, vol. 7, pp. 3635–3643, 2019.

[5] S.-G. Ha, J. Cho, E.-K. Kim, Y. B. Park, and K.-Y. Jung, "FDTD dispersive modeling with high-order rational constitutive parameters," *IEEE Trans. Antennas Propag.*, vol. 63, no. 9, pp. 4233–4238, Sep. 2015.

[6] J. Chen, G. Hao, and Q.-H. Liu, "Using the ADI-FDTD method to simulate graphene-based FSS at terahertz frequency," *IEEE Trans. Electromagn. Compat.*, vol. 59, no. 4, pp. 1218–1223, Aug. 2017.

[7] G. Xie, Z. Huang, M. Fang, and X. Wu, "A unified 3-D ADI-FDTD algorithm with one-step leapfrog approach for modeling frequency-dependent dispersive media," *Int. J. Numer. Model.*, to be published, doi: 10.1002/jnm.2666.

[8] A. Pereda, L. A. Vielva, A. Vegas, and A. Prieto, "Analyzing the stability of the FDTD technique by combining the von Neumann method with the Routh-Hurwitz criterion," *IEEE Trans. Microw. Theory Techn.*, vol. 49, no. 2, pp. 377–381, Feb. 2001.

[9] K. Y. Jung, F. L. Teixeira, and R. M. Reano, "Au/SiO_2 nanoring plasmon waveguides at optical communication band," *J. Lightw. Technol.*, vol. 25, no. 9, pp. 2757–2765, Sep. 1, 2007.

[10] J.-H. Kweon, M.-S. Park, J. Cho, and K.-Y. Jung, "FDTD analysis of electromagnetic wave propagation in an inhomogeneous ionosphere under arbitrary-direction geomagnetic field," *J. Electromagn. Eng. Sci.*, vol. 18, no. 3, pp. 212–214, Jul. 2018.

[11] A. Deinega and S. John, "Effective optical response of silicon to sunlight in the finite-difference time-domain method," *Opt. Lett.*, vol. 37, no. 1, pp. 112–114, Jan. 2012.

[12] K. P. Prokopidis and D. C. Zografopoulos, "A unified FDTD/PML scheme based on critical points for accurate studies of plasmonic structures," *J. Lightw. Technol.*, vol. 31, no. 15, pp. 2467–2476, Aug. 1, 2013.

[13] S.-G. Ha, J. Cho, J. Choi, H. Kim, and K.-Y. Jung, "FDTD dispersive modeling of human tissues based on quadratic complex rational function," *IEEE Trans. Antennas Propag.*, vol. 61, no. 2, pp. 996–999, Feb. 2013.

[14] H. Chung, J. Cho, S.-G. Ha, S. Ju, and K.-Y. Jung, "Accurate FDTD dispersive modeling for concrete materials," *ETRI J.*, vol. 35, no. 5, pp. 915–918, Oct. 2013.

[15] M. Han, R. W. Duttonm, and S. Fan, "Model dispersive media in finite-difference time-domain method with complex-conjugate pole-residue pairs," *IEEE Microw. Wireless Compon. Lett.*, vol. 16, no. 3, pp. 119–121, Mar. 2006.

[16] X. Du, H. Yu, and M. Li, "Effective modeling of tunable graphene with dispersive FDTD—GSTC method," *Appl. Comput. Electromagn. Soc. J.*, vol. 34, no. 6, pp. 851–857, Jun. 2019.

[17] I. T. Rekanos and T. G. Papadopoulos, "An auxiliary differential equation method for FDTD modeling of wave propagation in Cole-Cole dispersive media," *IEEE Trans. Antennas Propag.*, vol. 58, no. 11, pp. 3666–3674, Nov. 2010.

[18] A. Guellab and Q. Wu, "Modeling human body using four-pole Debye model in piecewise linear recursive convolution FDTD method for the SAR calculation in the case of vehicular antenna," *Int. J. Antennas Propaga.*, vol. 2018, Apr. 2018, Art. no. 2969237.

[19] H. Chung, S.-G. Ha, J. Choi, and K.-Y. Jung, "Accurate FDTD modelling for dispersive media using rational function and particle swarm optimisation," *Int. J. Electron.*, vol. 102, no. 7, pp. 1218–1228, Jul. 2015.

[20] T. Wuren, T. Takai, M. Fujii, and I. Sakagami, "Effective 2-Debye-pole FDTD model of electromagnetic interaction between whole human body and UWB radiation," *IEEE Microw. Wireless Compon. Lett.*, vol. 17, no. 7, pp. 483–485, Jul. 2007.

[21] B. Gustavsen and A. Semlyen, "Rational approximation of frequency domain responses by vector fitting," *IEEE Trans. Power Del.*, vol. 14, no. 3, pp. 1052–1061, Jul. 1999.

[22] *The Vector Fitting Web Site*. Accessed: Jun. 1, 2019. [Online]. Available: https://www.sintef.no/projectweb/vectfit/

[23] D. F. Kelley and R. J. Luebbers, "Piecewise linear recursive convolution for dispersive media using FDTD," *IEEE Trans. Antennas Propag.*, vol. 44, no. 6, pp. 792–797, Jun. 1996.

[24] D. M. Sullivan, "Z-transform theory and the FDTD method," *IEEE Trans. Antennas Propag.*, vol. 44, no. 1, pp. 28–34, Jan. 1996.

[25] M. Okoniewski, M. Mrozowski, and M. A. Stuchly, "Simple treatment of multi-term dispersion in FDTD," *IEEE Microw. Guided Wave Lett.*, vol. 7, no. 5, pp. 121–123, May 1997.

[26] E. L. Tan, "Efficient algorithms for Crank–Nicolson-based finite-difference time-domain methods," *IEEE Trans. Microw. Theory Techn.*, vol. 56, no. 2, pp. 408–413, Feb. 2008.

[27] S.-M. Park, E.-K. Kim, Y. B. Park, S. Ju, and K.-Y. Jung, "Parallel dispersive FDTD method based on the quadratic complex rational function," *IEEE Antennas Wireless Propag. Lett.*, vol. 15, pp. 425–428, 2016.

[28] D. Andreuccetti, R. Fossi, and C. Petrucci. *Dielectric Properties of Body Tissues*. Accessed: Jun. 1, 2019. [Online]. Available: http://niremf.ifac.cnr.it/tissprop/

[29] K. P. Prokopidis and D. C. Zografopoulos, "Investigation of the stability of ADE-FDTD methods for modified Lorentz media," *IEEE Microw. Wireless Compon. Lett.*, vol. 24, no. 10, pp. 659–661, Oct. 2014.
[30] C. A. Balanis, *Advanced Engineering Electromagnetics*. Hoboken, NJ, USA: Wiley, 1989.
[31] L. Han, D. Zhou, K. Li, X. Li, and W.-P. Huang, "A rational-fraction dispersion model for efficient simulation of dispersive material in FDTD method," *J. Lightw. Technol.*, vol. 30, no. 13, pp. 2216–2225, Jul. 1, 2012.
[32] K.-Y. Jung, B. Donderici, and F. L. Teixeira, "Transient analysis of spectrally asymmetric magnetic photonic crystals with ferromagnetic losses," *Phys. Rev. B, Condens. Matter.*, vol. 74, no. 16, pp. 165207-1–165207-11, Oct. 2006.
[33] M. Born and E. Wolf, *Principles of Optics*, 2nd ed. New York, NY, USA: Macmillan, 1964.

HONGJIN CHOI received the B.S. degree in mathematics from Hanyang University, Seoul, South Korea, in 2018, where he is currently pursuing the M.S. degree in electrical and computer engineering. His current research interests include computational electromagnetics and bioelectromagnetics.

YEON-HWA KIM received the B.S. degree in communication engineering from Daejin University, Pochen, South Korea, in 2018. She is currently pursuing the M.S. degree in electrical and computer engineering from Hanyang University, Seoul, South Korea. Her current research interests include computational electromagnetics and nanoelectromagnetics.

JAE-WOO BAEK received the B.S. degree in electronics and information engineering from Korea University, Sejong, South Korea, in 2015, and the M.S. degree in electrical and computer engineering from Hanyang University, Seoul, South Korea, in 2017, where he is currently pursuing the Ph.D. degree in electrical and computer engineering. His current research interests include computational electromagnetics, bioelectromagnetics, meta-surface electromagnetics analysis in THz, and parallel programming.

KYUNG-YOUNG JUNG (SM'13) received the B.S. and M.S. degrees in electrical engineering from Hanyang University, Seoul, South Korea, in 1996 and 1998, respectively, and the Ph.D. degree in electrical and computer engineering from The Ohio State University, Columbus, OH, USA, in 2008.

From 2008 to 2009, he was a Postdoctoral Researcher with The Ohio State University. From 2009 to 2010, he was an Assistant Professor with the Department of Electrical and Computer Engineering, Ajou University, Suwon, South Korea. Since 2011, he has been with Hanyang University, where he is currently an Associate Professor with the Department of Electronic Engineering. His current research interests include computational electromagnetics, bioelectromagnetics, and nano-electromagnetics.

Dr. Jung was a recipient of the Graduate Study Abroad Scholarship from the National Research Foundation of Korea, the Presidential Fellowship from The Ohio State University, the Best Teacher Award from Hanyang University, and the Outstanding Research Award from the Korean Institute of Electromagnetic Engineering Society.